Journal of Experimental Botany, Vol. 57, No. 10, pp. 2339–2351, 2006
doi:10.1093/jxb/erj205 Advance Access publication 23 June, 2006

Journal of Experimental Botany

RESEARCH PAPER

Purification, functional characterization, cloning, and identification of mutants of a seed-specific arabinan hydrolase in *Arabidopsis*

Zoran Minic[1], Cao-Trung Do[1], Christophe Rihouey[2], Halima Morin[1], Patrice Lerouge[2] and Lise Jouanin[1,*]

[1] *Laboratoire de Biologie Cellulaire – Institut National de la Recherche Agronomique, Route de St-Cyr, F-78026 Versailles Cedex, France*

[2] *Faculté des Sciences, UMR 6037 CNRS, IFRMP23, Université de Rouen, F-76821 Mont Saint Aignan Cedex, France*

Received 23 December 2005; Accepted 16 March 2006

Abstract

This work describes the purification and characterization of an enzyme that exhibits arabinan hydrolase activity in seeds of *Arabidopsis thaliana*. The enzyme, designated XYL3, had an apparent molecular mass of 80 kDa when purified to homogeneity, and was identified using MALDI-TOF (matrix-assisted laser desorption ionization–time of flight) as a putative β-D-xylosidase that belongs to family 3 of glycoside hydrolases encoded by gene *At5g09730*. XYL3 hydrolysed synthetic substrates such as *p*-nitrophenyl-α-L-arabinofuranoside and *p*-nitrophenyl-β-D-xyloside with similar catalytic efficiency. XYL3 released L-arabinose from (1→5)-α-L-arabinofuranobiose, arabinoxylan, sugar beet arabinan, and debranched arabinan. The enzyme hydrolysed both arabinosyl-substituted side group residues and terminal arabinofuranosyl residues (1→5)-α-linked to the arabinan backbone. This indicates that XYL3 is able to degrade all terminal arabinosyl residues and suggests that it participates in the *in-vivo* hydrolysis of arabinan. Analysis of gene expression patterns by semi-quantitative RT-PCR, *in-situ* hybridization and a promoter–GUS fusion demonstrated that *AtBX3* was specifically expressed in the seed endosperm at the globular stage of the embryo. Immunolocalization using LM6 anti-arabinan antisera found that arabinan, the XYL3 substrate, was also present in this seed tissue. T-DNA null mutants for *AtBX3* were identified. The mutant plants lacked the α-L-arabinofuranosidase and β-D-xylosidase activities corresponding to XYL3. Mutants showed reduced seed size and are delayed in seedling germination compared with the wild type.

Key words: *Arabidopsis thaliana*, arabinan, α-L-arabinofuranosidase, cell wall, endosperm, seed.

Introduction

The cell wall determines the size and shape of plant cells and undergoes morphological and compositional changes during plant growth and development (Stolle-Smits *et al*., 1999; Obel *et al*., 2002; Reiter, 2002). The remodelling of the cell wall structure is achieved by modifying polysaccharides, lignin, and proteins (Cosgrove, 1997; Stolle-Smits *et al*., 1999; Obel *et al*., 2002; Reiter, 2002; Boudet *et al*., 2003; Popper and Fry, 2003). Currently, increasing interest is being focused on the enzymes that mediate these modifications and in particular on their mode of action and substrate specificity. However, although numerous plant enzymes are involved in the structural modification and physical properties of cell wall polysaccharides, little information is available about them (Fry, 2004).

This study has focused on work on an *Arabidopsis* enzyme that hydrolyses L-arabinose (L-Ara) from cell wall polysaccharides. The monosaccharide L-Ara is an integral component of various cell wall polysaccharide polymers in higher plants such as the side chains of rhamnogalacturonan I, arabinoxylan, and arabinogalactan proteins (Bacic *et al*, 1988; Ridley *et al*, 2001; Glushka *et al*., 2003). L-Ara is

* To whom correspondence should be addressed. E-mail: jouanin@versailles.inra.fr

Abbreviations: L-Ara, L-arabinose; HPAE, high-performance anion-exchange; D-Xyl, D-xylose; MALDI-TOF, matrix-assisted laser desorption ionization–time of flight; *p*NP, *p*-nitrophenyl; *p*NPAf, *p*-nitrophenyl-α-L-arabinofuranoside; *p*NPX, *p*-nitrophenyl-β-D-xylopyranoside; SBA, sugar beet arabinan; SDS-PAGE, sodium dodecyl sulphate–polyacrylamide gel electrophoresis; WAX, wheat arabinoxylan; WT, wild type.

a major component of arabinan which is composed of a backbone of (1→5)-α-linked L-arabinofuranosyl residues branched with (1→3)-α-linked and (1→2)-α-linked side chains of L-Ara in the furanose conformation (Bacic *et al*., 1988; Rahman *et al*., 2003). In arabinoxylans, the (1→4)-β-D-xylose backbone is mainly branched with α-L-arabinofuranose residues linked in the α(1→3) position or, occasionally, in both α(1→3) and α(1→2) positions (Puls and Schuseil, 1993). Various enzymes can hydrolyse either backbone or side chains of arabinose-containing polysaccharides (Manin *et al*., 1994; Hazlewood and Gilbert, 1998; Saha, 2000). Among these, α-L-arabinofuranosidases (EC 3.2.1.55) are particularly important since they can cleave terminal non-reducing α-L-arabinofuranosyl groups from different arabinose-containing oligosaccharides and polysaccharides (Saha, 2000). They co-operate with endo-1,5-α-L-arabinases (EC 3.2.1.99), which act by carrying out endohydrolysis of (1→5)-α-L-arabinofuranosidic linkages in the arabinan backbone, resulting in their complete degradation.

All biochemically characterized plant α-L-arabinofuranosidases belong to glycosyl hydrolase families 3 or 51 (Ferré *et al*., 2000; Lee *et al*., 2001, 2003; Minic *et al*., 2004; Tateishi *et al*., 2005). To date, two α-L-arabinofuranosidases from family 51, which remove α-L-arabinofuranosyl residues from the arabinoxylan polymer, have been purified, sequenced, and characterized from barley (*Hordeum vulgare*) seedlings (Ferré *et al*., 2000; Lee *et al*., 2001). An α-L-arabinofuranosidase, from the same family, has also been purified from *Arabidopsis* stem tissue (Minic *et al*., 2004). This α-L-arabinofuranosidase can hydrolyse various natural substrates such as xylan, arabinoxylan, arabinan, and oligoxylan. In addition, it was recently reported that some putative β-D-xylosidases, which belong to glycosyl hydrolase family 3, also possess α-L-arabinofuranosidase activity (Lee *et al*., 2003; Minic *et al*., 2004). One of these, designated as ARA-I, has been purified, characterized, and sequenced from barley seedlings. ARA-I can degrade (1→5)-α-L-arabinofuranohexaose and (1→4)-β-D-xylopentaose (Lee *et al*., 2003). A second, XYL1, was purified and characterized from *Arabidopsis* stem tissue. XYL1 can degrade (1→4)-β-D-xylobiose and (1→4)-β-D-xylotetraose, and various natural substrates such as arabinoxylan, arabinan, oligoxylan, and oligoarabinoxylan (Minic *et al*., 2004). Recently, an α-L-arabinofuranosidase from family 3 expressed during Japanese pear fruit ripening was purified (Tateishi *et al*., 2005). This enzyme only released arabinose from native cell wall polysaccharides and sugar beet arabinan (SBA). Therefore, enzymes showing α-L-arabinofuranosidase activity from both families 3 and 51 of plant glycosyl hydrolases are capable of hydrolysing a variety of plant polysaccharides *in vitro*. However, their substrate specificity remains to be determined. Moreover, the functional differences between plant α-L-arabinofuranosidases from glycosyl hydrolases families 3 and 51 are not yet known.

In this paper, the purification, characterization, and identification of an enzyme, specifically expressed in the seed endosperm that exhibits α-L-arabinofuranosidase activity, are described. Its substrate specificity has been determined using various natural cell wall polysaccharides. Knockout mutants for the gene encoding this enzyme were obtained and characterized.

Materials and methods

Plant material

The ecotype Wassilewskija (WS) was used in this study. Wild-type (WT) WS *Arabidopsis* plants were grown in the greenhouse at 20–22 °C with a 16 h photoperiod at 150 μE m^{-2} s^{-1}. Mutants and WT *Arabidopsis* were grown together in the same greenhouse to ensure that the effects of environmental conditions were identical. The *Atbx*-3 mutants were selected using a systematic border sequencing program (http://flagdb-genoplante-info.infobiofen.fr) of the Versailles collection of T-DNA lines. T_3 homozygous mutant lines were selected on Estelle and Somerville medium (Estelle and Somerville, 1987) containing kanamycin (100 mg l^{-1}).

Chemicals

p-Nitrophenyl (*p*NP)-glycoside substrates, D-xylose (D-Xyl), L-Ara, *p*NP, and oat spelt xylan (approximately 10% L-Ara and 15% glucose residues) were purchased from Sigma (St Louis, MO, USA). (1→5)-α-L-Arabinobiose, wheat arabinoxylan (WAX), SBA, and linear (1→5)-α-linked debranched arabinan (88:4:2:6 L-arabinose–galactose–rhamnose–galacturonic acid) were purchased from Megazyme International (Bray, Ireland).

Preparation of protein extracts from Arabidopsis *tissues*

Tissue was harvested from *Arabidopsis* at the flowering stage. Approximately 2 g of tissue were suspended in 2 ml of ice-cold extraction buffer and blended for 5 min. The extraction buffer consisted of 25 mM BIS-TRIS, pH 7.0, 200 mM $CaCl_2$, 10% (v/v) glycerol, 4 μM Na-cacodylate, and 1/200 (v/v) protease inhibitor cocktail (P-9599; Sigma). The ground and suspended material was centrifuged twice at 4 °C for 3 min at 10 000 *g* and the supernatant was additionally centrifuged for 15 min at 17 000 *g*. The resulting supernatant was used for chromatographic analyses.

Chromatographic purification of enzymes exhibiting β-D-xylosidase activity

The protein extract obtained from flowers or siliques of WT *Arabidopsis* was used for purification of the enzyme. The purification was performed in five steps.

Step 1: *cation-exchange chromatography*: The soluble protein extract (5 mg protein in 2 ml) was equilibrated in 25 mM Na-acetate buffer (pH 5.0) containing 5% glycerol (v/v) and 0.015% Triton X-100 (v/v), and loaded on a CM-Sepharose (Sigma) cation-exchange column (1.5 cm×4 cm; Sigma). Glycerol was added to the buffer to prevent the partial enzymatic inactivation that was observed in its absence. The proteins were eluted with the same buffer, first alone and then with a 0.0–0.5 M NaCl discontinuous gradient using 2 ml of NaCl solution, increasing by 0.025 M. One-millilitre fractions were collected and 50 μl assayed for β-D-xylosidase activity. Peak fractions (23–27) showing β-D-xylosidase activity were pooled and used in the second step of purification.

Step 2: *lectin chromatography*: A 0.5 cm×3 cm column was filled with 1 ml of ConA Sepharose (Sigma) and washed with 3 ml of 20 mM TRIS-HCl, 0.5 M NaCl buffer (pH 7.4). The soluble protein

extract was loaded and then column washed with 10 ml of the buffer. The column was eluted with 0.2 M methyl-α-glucopyranoside in the same buffer. The eluates were collected (0.5 ml per fraction) and 50 µl samples from each fraction were tested for β-D-xylosidase activity as described below.

Step 3: *gel-filtration chromatography*: Pooled fractions 12–15 showing β-D-xylosidase activity after step 2 were concentrated to 500 µl and fractionated by fast protein liquid chromatography (Pharmacia) on a Superdex 200 HR10/30 column (Amersham Pharmacia Biotech), pre-calibrated with the following markers of known molecular mass: thyroglobulin (670 kDa), bovine gamma globulin (158 kDa), chicken ovalbumin (44 kDa), equine myoglobin (17 kDa), and vitamin B_{12} (1.35 kDa). Equilibration and elution were performed at room temperature with 20 mM Na-acetate buffer (pH 5.0), containing 150 mM NaCl. Fractions of 0.4 ml were collected at a flow rate of 0.5 ml min^{-1}, and 50 µl of each fraction were assayed for β-D-xylosidase activity. Fractions 11–13 exhibiting this activity were pooled and dialysed against 25 mM TRIS-HCl buffer (pH 7.4), in the presence of 5% glycerol (v/v).

Step 4: *anion-exchange chromatography*: The dialysed fractions (1.2 ml) were loaded on a DEAE Sephacel (Sigma) anion-exchange column (1.5 cm×4 cm; Sigma). Proteins were eluted with 25 mM TRIS-HCl buffer (pH 7.4), first alone and then in a 0.0–0.4 M NaCl discontinuous gradient as described in step 1. One-millilitre fractions were collected and 100 µl assayed for β-D-xylosidase activity.

Step 5: *chromatofocusing*: Fractions 8–11 showing β-D-xylosidase activity from step 4 were pooled and concentrated to 1 ml, and equilibrated in 25 mM ethanolamine buffer, pH 9.4, and applied to a column (0.9 cm×15 cm) of Polybuffer exchangers PBE 94 resin (Amersham Biosciences) equilibrated in the same buffer. Elution was performed with Polybuffer 96, 10-fold diluted with distilled water, and adjusted to pH 6.0. Fractions of 0.5 ml were collected. A single peak of β-D-xylosidase was observed at pH 7.5. Peak fractions 26–28 were pooled and concentrated to 100 µl, then used for biochemical analysis.

Sodium dodecyl sulphate–polyacrylamide gel electrophoresis (SDS-PAGE)

Protein-denaturing SDS-PAGE was carried out using 10% polyacrylamide gels (Laemmli, 1970). Standard markers (molecular weight range 15–150 kDa; M 0671; Sigma) were used to determine the approximate molecular masses of purified proteins in gels stained with Coomassie Brilliant Blue R-250.

Identification of proteins by mass spectroscopy

The purified protein was digested with trypsin according to the conditions described by Santoni *et al*. (2003). Tryptic peptides were analysed by matrix-assisted laser desorption ionization–time of flight (MALDI-TOF) mass spectrometry on a REFLEX III instrument (Bruker Instruments, Billerica, MA, USA). Finally, proteins were identified using Mascot (http://www.matrixscience.com/).

β-D-Xylosidase and α-L-arabinofuranosidase activity assays

The reaction mixture contained 2 mM *p*-nitrophenyl-β-D-xylopyranoside (*p*NPX) (Sigma) or 2 mM *p*-nitrophenyl-α-L-arabinofuranoside (*p*NPAf) (Sigma-Aldrich, St Louis, MO, USA), 0.1 M Na-acetate buffer (pH 5.0) and 50–100 µl of protein extract in a total volume of 0.5 ml (Goujon *et al*., 2003). The reaction was carried out at 37 °C for 60 min and stopped by the addition of 0.5 ml of 0.4 M sodium bicarbonate to the assay mixture. Staining intensity was determined spectrophotometrically at 405 nm, and the amount of the resulting *p*-nitrophenol was determined from a calibration curve. One unit of activity is defined as the amount of enzyme releasing 1 µmol of *p*-nitrophenol min^{-1}, as measured by absorbance at 405 nm. The activity toward other *p*NP-glycosides was determined as described above for β-D-xylosidase or α-L-arabinofuranosidase.

Time-course of hydrolysis of polysaccharides by the purified enzymes

For the time-course of polysaccharide hydrolysis, the reaction mixture contained 0.1 µg of purified enzyme in 0.5 ml of 25 mM Na-acetate buffer (pH 5.0) containing 2% (w/v) of polysaccharide. For the control reaction no protein extract was added. Reactions were incubated at 37 °C for specific times and then boiled for 3 min to stop the reaction. The mixture was then centrifuged at 17 000 *g* for 5 min and the supernatant used for analysis.

Cleavage products were fractionated using a high-performance anion-exchange (HPAE) chromatographic system (Dionex X500) equipped with a CarboPac PA-1 column, and combined with pulse amperometric detection. Degradation products were quantified by the integration of peak areas as described previously (Minic *et al*., 2004). The concentrations of released L-Ara and D-Xyl were determined from a calibration curve. The standard deviation values for three replicate assays were <6%.

pH and temperature profiles

The determination of temperature dependence was carried out at pH 5.0 as described above for the β-D-xylosidase and α-L-arabinofuranosidase assays, except that the temperature ranged from 30 °C to 70 °C. To determine the pH optimum, the temperature was 37 °C and the pH varied from 3.0 to 8.0 in 100 mM Na-acetate/citrate buffer.

Kinetic analyses

Kinetic parameters of purified enzymes were determined for the substrate *p*NPX in a concentration range of 0.05–4.0 mM and of 0.2–8.0 mM for *p*NPAf and (1→5)-α-L-arabinobiose substrates, respectively. Assays were performed in 100 mM Na-acetate buffer, pH 5.0. Standard deviation values for assays were <5%. Kinetic data were processed using Kaleidagraph program (Synergy Software, Reading, PA, USA) based on Michaelis–Menten enzyme kinetics (Atkins and Nimmo, 1980).

mRNA expression

Total RNA was extracted from different *Arabidopsis* tissues using Trizol (Qiagen USA, Valencia, CA, USA) and used for semi-quantitative RT-PCR experiments. Primers P3f (5′-CAAGGCGGG-TTTGGTAA-3′) and P3r (5′-GGCGAATGTAATCTCAAATC-3′) were used to amplify the *AtBX*3 cDNA. A control RT-PCR was performed with the same cDNA with the β-tubulin gene *At5g44340* using the primers 5′-GTCCAGTGTCGTGATATTGCAC-3′ and 5′-GCTTACGAATCCGAGGGTGCC-3′.

In-situ *hybridization*: Antisense transcripts for *AtBX3* cDNA were synthesized and labelled *in vitro* with digoxigenin-11-UTP using T7 RNA polymerase (Promega Kit, Madison, MI, USA). *In-vitro* transcription reactions were performed following the manufacturer's protocol, except that the ratio of labelled to unlabelled UTP was 1:1.

The template for the transcription of *AtBX3* antisense probes was derived from a PCR-amplified 626 bp cDNA fragment using an *AtBX*3-specific primer (5′-TGTAATACGACTCACTATAGGGCG-AATGTAATGTCAAAT-3′) and a T7-specific primer. Tissues were fixed, dehydrated, and embedded according to the method of Lincoln *et al*. (1994), except that hybridization with the *AtBX3* probe was performed at 45 °C and the final wash was performed in 2× SSC (sodium chloride/sodium citrate), 50% formamide at 45 °C. Immunological detection was carried out as described by Coen *et al*. (1990).

AtBX3 *promoter::GUS fusion*

Genomic DNA from *Arabidopsis thaliana*, ecotype WS, was used to amplify the PCR fragment including the promoter region of *AtBX3*

using primers RBX3 (5′-GACGCATCTAGACACTAACCACAT-CATGATATGC-3′) and LBX3 (5′-ATGAGCGCCTAGGCGATT-GTTCGATTGCTCGGAGA-3′) including *Xba*I and *Bam*HI sites, respectively. This *AtBX3* fragment was subcloned upstream of the *GUS*-coding region in pBI101.2 (Clontech, Palo Alto, CA, USA) after *Xba*I/*Bam*HI digestion. The resulting construct contained a 1048 bp region upstream of the *AtBX3* translational start site, and an 85 bp coding region fused in-frame to the *uid*A gene.

Immunolocalization of arabinan

The samples for immunofluorescence microscopy were prepared using the method of Baluska *et al*. (1992). Briefly, young siliques were cut and fixed in 4% formaldehyde in PBS (phosphate-buffered saline) pH 6.9 for 1 h at room temperature under vacuum.

The siliques were dehydrated in a graded ethanol series (30–97% ethanol in PBS) then incubated in wax:ethanol (1:2, 1:1, and 2:1 steps) and finally infiltrated in 100% Steedman's wax [PEG-400 distearate and 1-hexadedecanol, 9:1 (w/w)] at 40 °C. The infiltrated siliques were then embedded by allowing the wax to polymerize at room temperature.

Longitudinal sections (12 μm thick) were cut with a microtome and mounted on slides. The sections were dewaxed in 100% ethanol, rehydrated in an ethanol series (97–50% ethanol in PBS), and finally washed with PBS. For immunostaining, the sections were incubated with BSA (bovine serum albumin) (1% w/v) to block non-specific binding sites for 30 min, and the labelling with the primary monoclonal antibody anti(1→5)-α-L-arabinan (LM6; Willats *et al.*, 1998) (Plant Probes™, Leeds, UK) was added at 10-fold dilution in PBS/BSA for 2 h. After washing with PBS, the sections were incubated with a secondary goat anti-rat-IgG antibody conjugated to Alexa Fluor® 488 (Molecular Probes™, Invitrogen, Cergy Pontoise, France) diluted 500-fold for 1 h at room temperature. The labelled sections were viewed with a confocal laser scanning microscope (Leica SP2 AOBS, Germany™).

Molecular characterization of the mutants

Genomic DNA was extracted from the leaves of WT and mutant plants as described by Doyle and Doyle (1990). PCR was performed in standard conditions (Sambrook *et al*., 1989) using primers flanking the T-DNA insertion (P1f, 5′-CCCAACACTCTCAAGCAA-3′; P1r, 5′-CAAACCRGCCAATAGAGA-3′; P2f, 5′-ATGTGTGAAACT-GAGATTG-3′; P2r, 5′-TGGTCGAATTTAGTGTAGG-3′).

Bioinformatic analyses

Sequences were aligned using the FASTA program (http://fasta.bioch.virginia.edu/fasta/align.htm) (Corpet, 1988). Cleavage and glycosylation sites of deduced proteins were studied using PSORT and NetNGlyc software (Nielsen *et al*., 1997; Nakai and Horton, 1999) at http://psort.nibb.ac.jp/form.html and http://www.cbs.dtu.dk/services/NetNGlyc/.

Protein measurements

Protein concentrations were determined as described by Bradford (1976) using the Coomassie Brilliant Blue method with BSA as a standard.

Results

Elution profile of β-D-xylosidase activities after cation exchange chromatography on CM-Sepharose in various Arabidopsis *tissues*

Seven putative xylosidase genes, which encode proteins that are phylogenetically related to β-D-xylosidases, have been identified in the genome of *Arabidopsis* (Goujon *et al*., 2003). Enzymatic properties have been studied for two of these enzymes (XYL1 and XYL4). These enzymes were purified and identified from *Arabidopsis* stem tissue (Minic *et al*., 2004). In order to identify other β-D-xylosidases, this activity was examined in various *Arabidopsis* tissues. Protein extracts from various *Arabidopsis* tissues (stem, roots, leaves, flowers, and siliques) were fractionated by cation-exchange chromatography on CM-Sepharose, and pooled fractions were assayed for β-D-xylosidase activity. Three major peaks (I, II, and III) of activity were present in different proportions in several tissues as shown in Fig. 1. Peaks I and III obtained from stem extracts corresponded to previously purified and characterized XYL1 and XYL4 enzymes (Minic *et al*., 2004). In addition, one major peak (II) of high β-D-xylosidase activity was observed in flower and silique tissue (Fig. 1). The elution position of this peak was different from the position of the peaks observed in stem tissue. This new peak, therefore, corresponded to an unknown β-D-xylosidase in *Arabidopsis*.

Purification of an enzyme with high β-D-xylosidase activity in Arabidopsis *flower and silique tissues*

The enzyme was purified by monitoring β-D-xylosidase activity using *p*NPX as a substrate. Table 1 indicates the degree of purification and yield for each step. The purification protocol involved five steps of column chromatography: in the first step a major peak of activity was eluted from a CM-Sepharose column (Fig. 1). Pooled fractions showing β-D-xylosidase activity were loaded onto a ConA Sepharose column. Resulting fractions with β-D-xylosidase activity were purified by gel filtration on Superdex 200. The pooled fractions with β-D-xylosidase activity from this step were

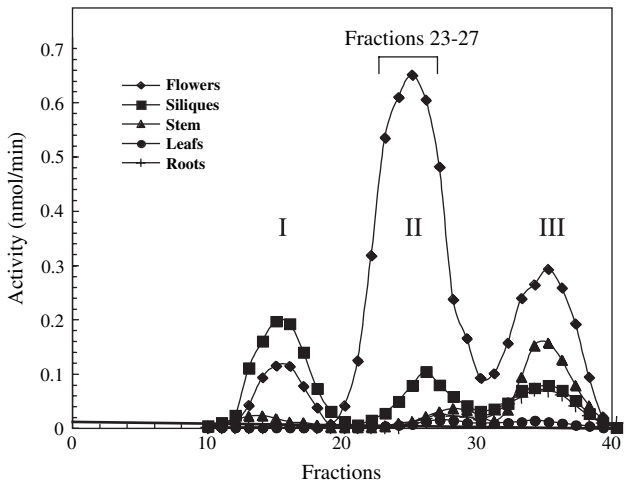

Fig. 1. Elution profile of β-D-xylosidase activity in CM-Sepharose cation-exchange chromatography using protein extracts from various tissues of *Arabidopsis*. A 2 ml dialysed cell-free extract was eluted as described for purification step 1 (see Materials and methods). The first 10 fractions were not analysed in enzymatic assays since these fractions contained pigments which show high absorbance at 405 nm.

Table 1. *Enzyme yields and purification factors for Peak II*

Step of purification	Yield		Specific activity (mU mg^{-1})	Recovery (%)[a]	Purification factor (fold)[a]
	Protein (mg)	Activity (mU)			
Crude homogenate	5.0	51.00	10.2	100	1
CM-Sepharose	0.920	29.00	31.5	56.9	3.1
ConA Sepharose	0.213	11.37	53.4	22.3	5.2
Superdex 200	0.054	5.41	100.2	10.6	9.8
DEAE-Sephacel	0.016	3.02	188.8	5.9	18.5
Chromatofocusing	0.005	1.08	216.0	2.1	21.2

[a] Recoveries are expressed as percentage of initial activity and purification factors are calculated on the basis of specific activities.

further purified using anion exchange chromatography on DEAE Sephacel (Table 1). Finally, the active fractions obtained after DEAE-Sephacel chromatography were applied to a column of PBE resin, and a single peak of β-D-xylosidase activity was observed. The active fractions were pooled, concentrated, and used for biochemical analysis. Through all the purification steps, elution profiles of β-D-xylosidase activity corresponded to those with α-L-arabinofuranosidase activity (data not shown).

SDS-PAGE analysis of the isolated enzyme

The purity of the protein isolated after chromatofocusing was examined by SDS-PAGE. Staining with Coomassie Brilliant Blue R-250 revealed only one band (Fig. 2). The apparent molecular mass of the protein was 80 kDa. In addition, Superdex 200 chromatography of the purified protein suggested that it is a native monomer since it was eluted at a position corresponding to a molecular mass similar to that determined on denaturing SDS-PAGE (data not shown).

Identification of the purified enzyme

In order to identify the enzyme, the purified protein was digested with trypsin and then analysed by MALDI-TOF using 'Mascot' algorithms. The enzyme was identified as a putative β-D-xylosidase, encoded in the *Arabidopsis* genome by the gene *At5g09730* and named *AtBXL3* in Goujon *et al*. (2003) (accession number T49925 in the BLAST databank). This enzyme was designated as XYL3. N-terminal amino acid sequencing of the first eight residues of the purified enzyme confirmed amino acid identity with AtBXL3 (Fig. 3).

Analysis of the primary structure of the purified enzyme

A BLAST sequence-similarity search revealed that the XYL3 protein showed 76% amino acid sequence identity with XYL4 β-D-xylosidase from *Arabidopsis* (Minic *et al*., 2004), 62% with ARA-I bifunctional α-L-arabinofuranosidase/β-D-xylosidase from barley (Lee *et al*., 2003), and 55% with XYL1 bifunctional α-L-arabinofuranosidase/β-D-xylosidase from *Arabidopsis* (Minic *et al*., 2004). The bioinformatic analysis using PSORT predicts the existence of a 23 amino acid signal sequence (Fig. 3). This predicted NH_2-terminus residue of XYL3 was experimentally confirmed by Edman sequence analysis. This analysis showed that the NH_2 terminal was the Glu residue of the EQSNNQSS sequence. The molecular mass calculated from the XYL3 sequence after removal of the NH_2-terminal signal sequences is 80.6 kDa (Fig. 3). This value corresponds well with that obtained by SDS-PAGE (Fig. 2). Finally, XYL3 possesses five potential sites for *N*-glycosylation (Fig. 3).

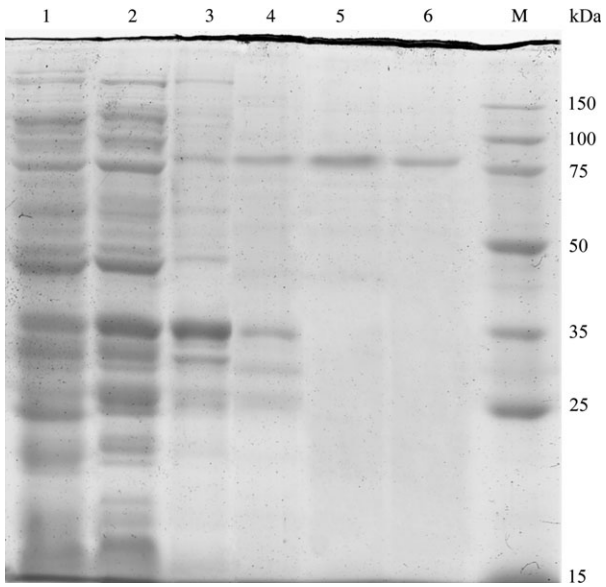

Fig. 2. SDS-PAGE of protein fractions during the purification of XYL3: lane 1, seedling homogenate (40 μg); lane 2, CM-Sepharose pooled fractions (40 μg); lane 3, ConA Sepharose-pooled fractions (10 μg); lane 4, Superdex 200-pooled fractions (5 μg); lane 5, DEAE Sephacel-pooled fraction (3 μg), lane 6, purified XYL3 after Polybuffer Exchanger 94 chromatography (1.5 μg); lane M, marker proteins (molecular masses are indicated, 10 μg).

Determination of the purified enzyme substrate specificities using p*NP-glycosides*

To determine the substrate specificity of XYL3, its enzymatic activity was tested using various artificial *p*NP-glycosides and natural substrates. On the basis of the results reported in Table 2, the purified enzyme showed activity for *p*NPAf and for *p*NPX. Similar results were previously observed for α-L-arabinofuranosidase from *Arabidopsis* and for bifunctional α-L-arabinofuranosidase/β-D-xylosidases

Fig. 3. Amino acid sequences of XYL3. The starting NH_2-terminal residue, after removal of the signal sequence, is indicated by an arrowhead. A bold overline shows the peptide sequence confirmed by NH_2-terminal Edman analysis. Overlines indicate peptide sequences obtained by MALDI-TOF after proteolytic cleavage by trypsin. Asterisks indicate potential *N*-glycosylation sites. Arrows indicate the putative catalytic nucleophiles (Asp298) and putative catalytic acid/bases (Glu502).

Table 2. *Relative activity of XYL3 with different substrates*

Aryl glycosides were used as substrates with purified proteins (0.1 μg) in standard assays at a final concentration of 4 mM. Activities were expressed as the percentage of activity compared with the maximal substrate activity obtained (100% of activity is equivalent to 65 μU). No activity was detected for *p*NP-β-D-fucopyranoside, *p*NP-β-D-glucopyranoside, *p*NP-α-D-glucopyranoside, *p*NP-β-L-arabinopyranoside, Me-β-D-xylopyranoside, *p*NP-α-D-xylopyranoside, *p*NP-α-D-fucopyranoside, *p*NP-β-D-mannopyranoside, *p*NP-α-D-mannopyranoside, and *p*NP-β-D-glucuronide.

Substrate	Relative activity (%)
*p*NP-α-L-arabinofuranoside	100
*p*NP-β-D-xylopyranoside	34
*o*NP-β-D-xylopyranoside	15
*p*NP-β-L-arabinopyranoside	3
*p*NP-α-D-galactopyranoside	2
*p*NP-β-D-galactopyranoside	3

isolated from *Arabidopsis* (Minic *et al*., 2004) and from barley (Lee *et al*., 2003). In addition to *p*NPX and *p*NPAf, the purified XYL3 could hydrolyse other substrates, such as *p*-nitrophenyl-β-D-galactopyranoside, *p*-nitrophenyl-α-D-galactopyranoside, and *p*-nitrophenyl-α-L-arabinopyranoside, but less efficiently (Table 2).

Kinetic properties and enzymatic characterization obtained using NP-glucosides

To confirm the bifunctional specificity of XYL3, its catalytic efficiency towards *p*NPAf and *p*NPX substrates was tested. The k_{cat}/K_m ratios obtained were 7.33 mM^{-1} s^{-1} and 5.23 mM^{-1} s^{-1} for *p*NPAf and *p*NPX, respectively. Indeed the small difference in k_{cat}/K_m ratios suggests that XYL3 acts as bifunctional α-L-arabinofuranosidase/β-D-xylosidase (Table 3A). Purified XYL3 showed an approximately 3-fold higher k_{cat}/K_m with *p*NPX than ARAf which had been purified recently from *Arabidopsis* stem tissue (Minic *et al*., 2004). The exact K_m value of ARAf against *p*NPAf was not determined because *p*NPAf could not be dissolved at concentrations higher than 15 mM.

The influence of pH on the activity of the enzyme was investigated between pH 3 and pH 8. The pH optima determined for XYL3 was 4.7. The temperature dependence of XYL3 activity was tested between 20 °C and 75 °C, and the apparent optimum temperature was 65 °C.

Enzyme activities of XYL3 towards the synthetic *p*-nitrophenol glycosides were similar to those observed for α-L-arabinofuranosidase (ARAf).

Hydrolysis of xylopolysaccharides, arabinan, and arabinobiose by XYL3

In order to determine eventual functional differences between XYL3 (family 3 of glycosyl hydrolases) and ARAf (family 51 of glycosyl hydrolases), their hydrolysis efficiency towards natural plant polysaccharides that contain L-Ara and D-Xyl was compared. Incubation of the purified enzyme with xylopolysaccharides and arabinan was carried

Table 3A. *Kinetic parameters of XYL3 and ARAf using pNPX and pNPAf as substrates*

Assays were performed using 0.1 μg of purified protein.

Substrate	K_m (37 °C) (mM)	k_{cat} (s^{-1})	k_{cat}/K_m (mM^{-1} s^{-1})
*p*NPX	0.26	1.36	5.23
*p*NPAf	3.52	25.28	7.33

out to determine if it could degrade native plant polysaccharides. Neoformed products were analysed by HPAE and compared with those released by ARAf. The time-course of polysaccharide hydrolysis is shown in Fig. 4. The results obtained indicate that both XYL3 and ARAf release D-Xyl in a similar ratio from WAX (Fig. 4A) and oat spelt xylan; data not shown). The release of L-Ara from WAX by ARAf is more efficient than the release by XYL3 (Fig. 4B). The highest production of L-Ara by XYL3 was observed using SBA as a substrate (Fig. 4C), whereas ARAf gives low yields of L-Ara from this substrate. Thus, the degradation activities of the two enzymes on wheat arabinoxylan were the opposite of their activities on SBA. Moreover, both enzymes degraded debranched α(1→5)-L-arabinan backbones (Fig. 4D).

To confirm the difference in the functional specificity of XYL3 and ARAf, their catalytic efficiencies were tested with (1→5)-α-L-arabinobiose as a substrate; the results of this experiment are shown in Table 3B. The k_{cat}/K_m ratios obtained were 2.92 mM^{-1} s^{-1} and 6.08 mM^{-1} s^{-1} for ARAf and XYL3, respectively. Thus, the k_{cat}/K_m ratio of XYL3 towards arabinobiose was higher than that of ARAf.

These results indicate that XYL3 and ARAf have similar specificities towards synthetic substrates such as *p*NPX and *p*NPAf, but different specificities towards the natural polysaccharides tested. By contrast to ARAf, which prefers arabinoxylan as a substrate, XYL3 has a preference for the arabinan substrates tested (SBA, debranched arabinan, and arabinobiose). In conclusion, the purified enzyme XYL3 was found to possess arabinose-releasing activity on a variety of arabinose-containing substrates.

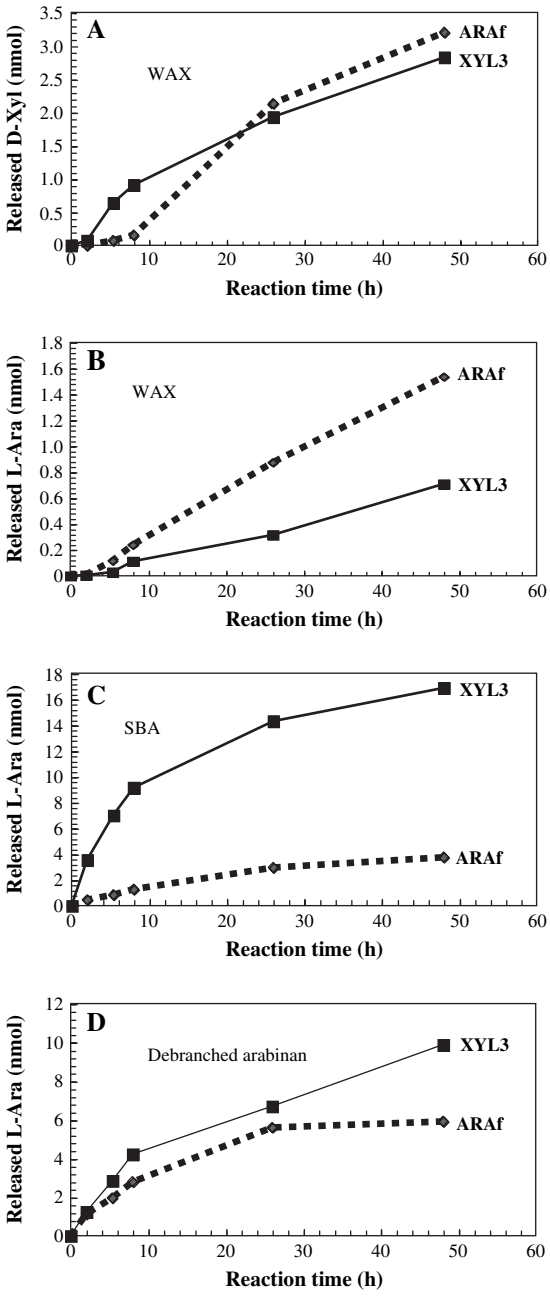

Fig. 4. Time-course of hydrolysis of WAX, SBA, and debranched arabinan by XYL3 and ARAf. A reaction mixture containing 0.1 μg of enzyme, 2% substrate (w/v) in 25 mM Na-acetate buffer, pH 5.0, was incubated at 37 °C for different time periods. Aliquots were taken at different intervals and boiled for 3 min to inactivate the enzyme followed by quantification of the reaction products with high-performance anion-exchange (HPAE) chromatography (Dionex X500) equipped with a CarboPac PA-1 column combined with pulse amperometric detection. (A) Release of D-xylose from arabinoxylan; (B) release of L-arabinose from arabinoxylan; (C) release of L-arabinose from arabinan; (D) release of L-arabinose from debranched arabinan.

AtBX3 *expression is seed specific*

Expression profile determined by RT-PCR: To determine the precise transcriptional expression profile of *AtBX3*, the gene encoding XYL3, total RNA was extracted from different organs of *Arabidopsis* (plantlets, floral stems, rosette leaves, cauline leaves, roots, flowers, and siliques) and used for RT-PCR experiments. The transcript was observed in flowers and siliques (Fig. 5A). In order to determine the precise stage of expression in flower and silique formation, RNA of 12 different flower/silique developmental stages (st) were used in RT-PCR. *AtBX3* signal was observed in the first three stages which correspond to closed buds, and flowers with stamens protruding from the flowers by 2 mm and by 5 mm, respectively. Highest expression levels were observed at the 2 mm stage (Fig. 5B for stages 0–4; latter stages not shown). The *AtBX3* signal was high in seeds 4 d after pollination, very low in seeds 9 d after

Table 3B. *Kinetic parameters of XYL3 and ARAf using (1→5)-α-L-arabinobiose as substrate*

Assays were performed using 0.1 μg of purified protein.

Enzyme	K_m (37 °C) (mM)	k_{cat} (s^{-1})	k_{cat}/K_m (mM^{-1} s^{-1})
XYL3	5.5	33.47	6.08
ARAf	5.2	15.20	2.92

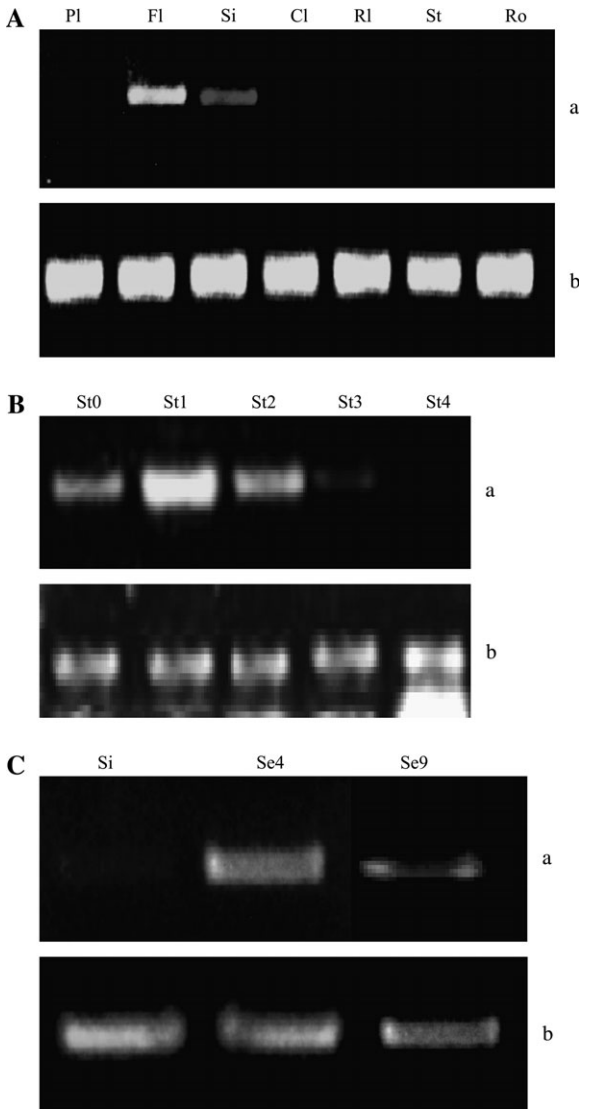

Fig. 5. Expression profiles of the *AtBX3* gene. Semi-quantitative expression was determined using reverse-transcription (RT)-PCR. (A) *AtBX3* detection in different organs of *Arabidopsis* (Pl, plantlets; Fl, flowers; Si, siliques; Cl, cauline leaves; Rl, rosette leaves; St, floral stem; Ro, roots). (B, C) *AtBX3* detection in different stages of flower and silique formation (St0, closed bud; St1, flowers with stamens sticking out of flowers by 2 mm; St2, flowers with stamens sticking out of flowers by 5 mm; St3, flowers fading, St4, developing siliques; Si, silique envelops 4 d after pollination; Se4 and Se9, isolated seeds 4 d and 9 d after pollination, respectively). a, Amplification with *AtBX3*-specific primers; b, amplification with β-tubulin-4-specific primers (β-tubulin-4 is a gene considered as constitutively expressed).

pollination, and not observed in silique envelopes at 4 d after pollination (Fig. 5C, and not shown). *AtBX3* expression was not detected in mature embryos, testa, and in silique envelopes (green mature stage; data not shown). In conclusion, *AtBX3* mRNA was specifically expressed in the early stage of seed formation and not at seed maturation.

Expression profile determined by in situ *hybridization*: In order to localize precisely the expression in the seeds, *in situ* hydridization was performed on developing seeds of *Arabidopsis* at different stages of development using an *AtBX3* probe. A high hydridization signal was observed exclusively in the endosperm of very young seeds when the embryo was at the globular stage (Fig. 6A). No signal was observed in the older stages of seed development. The specificity of the observed hybridization signal was demonstrated by the lack of hybridization in seeds of a knock-out mutant for the gene encoding AtBX3 (see below) at the same stage of development (Fig. 6B).

Expression profile determined by promoter–GUS *fusion*: The promoter region of *AtBX3* was fused to the coding sequence of the β-glucuronidase gene and introduced in *Arabidopsis*. The GUS-activity profile was determined in several transformed plants. No expression was detected in the vegetative parts (roots, leaves, stems) of the transgenic plants (data not shown). The GUS expression was restricted to very young siliques in development. Microscopic observation of cross-sections of seeds at the globular stage showed that the GUS staining was specific to the endosperm at this stage (Fig. 6C).

Presence of arabinan in Arabidopsis *seeds*

The *in vitro* activity tests of XYL3 suggested a high affinity for arabinan. The monoclonal antibody LM6 specific to arabinan was used to look for the presence of this polysaccharide in the endosperm of seeds in development. The observed labelling was restricted to the endosperm and outer integument, demonstrating the presence of pectin with arabinan side chains in *Arabidopsis* seeds (Fig. 6D).

Isolation and characterization of AtBX3 *mutants*

To define the role of XYL3 further, two null mutant lines were identified for the *AtBX3* gene in the Versailles T-DNA insertion collection (Bouché and Bouchez, 2001). These lines (named *Atbx3a* and *Atbx3b*) were identified by systematic border sequencing (http://flagdb-genoplante-info.infobiogen.fr). The segregation of progeny of these lines, germinated on selective medium containing kanamycin, allowed the inference that only one *npt*II insertion locus was present in each line. The sites of the insertions were localized in the fourth and sixth exons, respectively (Fig. 7).

Homozygous lines were obtained and the impact of the T-DNA insertion on mRNA expression was determined by RT-PCR on total RNA from flowers. The absence of *AtBX3* mRNA was confirmed in *Atbx3a* and *Atbx3b* (data not shown).

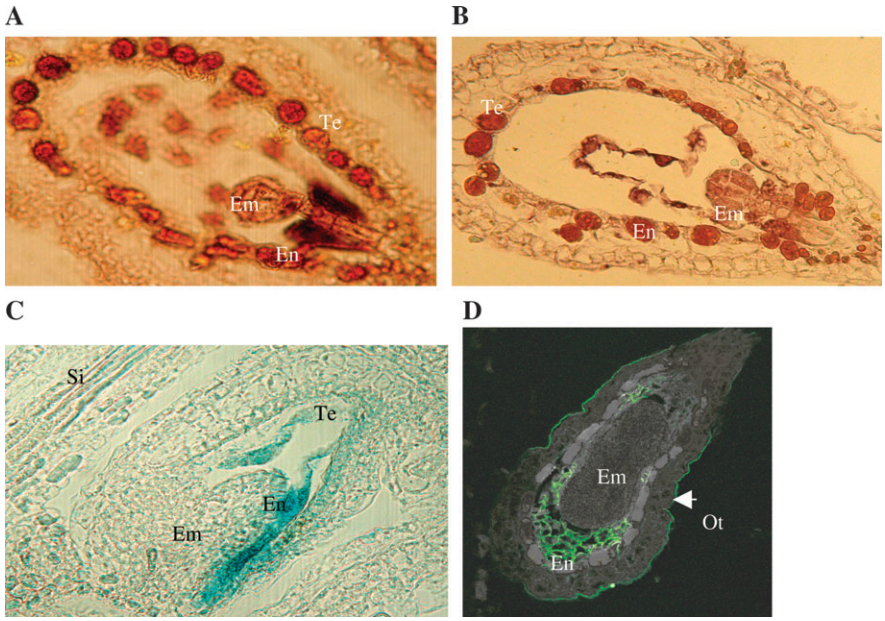

Fig. 6. (A, B) *In situ* hybridization performed on developing seeds. The selected photos present the seeds with globular-stage embryos corresponding to the stage when this gene is expressed in the endosperm: (A) the probe corresponds to the antisense transcript of *AtBX3*; (B) the control corresponds to the same hybridization performed on seeds of a knockout mutant for this gene (see Materials and methods for details of how the mutant was obtained). (C) Expression of *AtBX3*::*GUS* in the seed. A GUS assay was performed on an immature seed harvested from a transgenic line harbouring the *AtBX3* promoter fused to the *uid*A gene. The GUS staining was restricted to the endosperm. (D) Immunolocalization of arabinan in *Arabidopsis* seed. LM6 antiserum was used to localize the pectin arabinan side chain in immature seeds. The presence of arabinan is revealed by the green staining of the endosperm and the outer integument. Em, Embryo; En, endosperm; Ot, outer tegument; Si, silique; Te, testa.

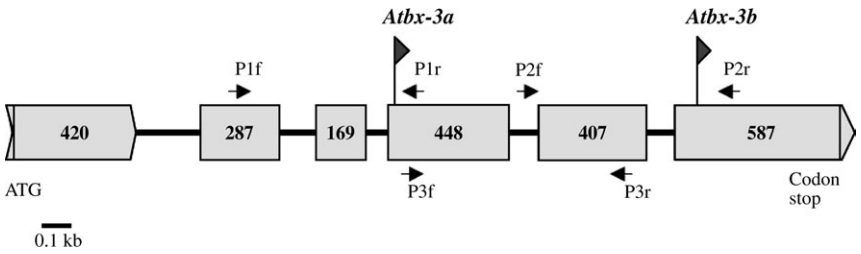

Fig. 7. Schematic representation of the *AtBX3* gene and localization of the T-DNA insertions in each T-DNA line. The numbers of nucleotides are indicated in the white rectangles representing each exon. The position of the T-DNA insertion for each mutant is indicated by flags. The position of the primers used to identify the mutant lines (P1f and P1r, P2f and P2r for *Atbx3a* and *Atbx3b*, respectively) and to verify the absence of mRNA expression in the mutant lines (P3f and P3r) are indicated by arrows.

The homozygous mutant lines and WT *Arabidopsis* were cultivated at the same time in greenhouse conditions. β-D-Xylosidase and α-L-arabinofuranosidase activities were determined in flowers of the mutant lines and the peak corresponding to XYL3 was absent from mutant extracts (Fig. 8) for *Atbx3a* (data not shown for *Atbx3b*). No obvious phenotype was observed for growth parameters on the two mutant lines when compared with the WT. However, siliques of the mutant lines were smaller than those of WT and, inside, the seeds were smaller in size than WT seeds (Fig. 9). The size of mature dried seeds was also slightly reduced but the weight was not reduced (Table 4). In addition, mutant seed germination rates were lower, as 5 d after sowing only 70.5% of seeds had germinated compared with 91.5% of WT seeds. However, all the mutant seeds were able to germinate later and no delay in plantlet development was noticed.

Discussion

In this study, a novel enzyme with arabinan hydrolase activity, named XYL3, was purified and characterized from *Arabidopsis thaliana*. XYL3 belongs to glycosyl hydrolase family 3. This is the first investigation that describes a plant hydrolytic enzyme that can degrade both arabinan and debranched arabinan, thus showing complete arabinan hydrolytic activity.

XYL3 has a pH optimum and K_m similar to previously characterized plant α-L-arabinofuranosidases from glycosyl hydrolase families 3 and 51, such as ARA-I from barley

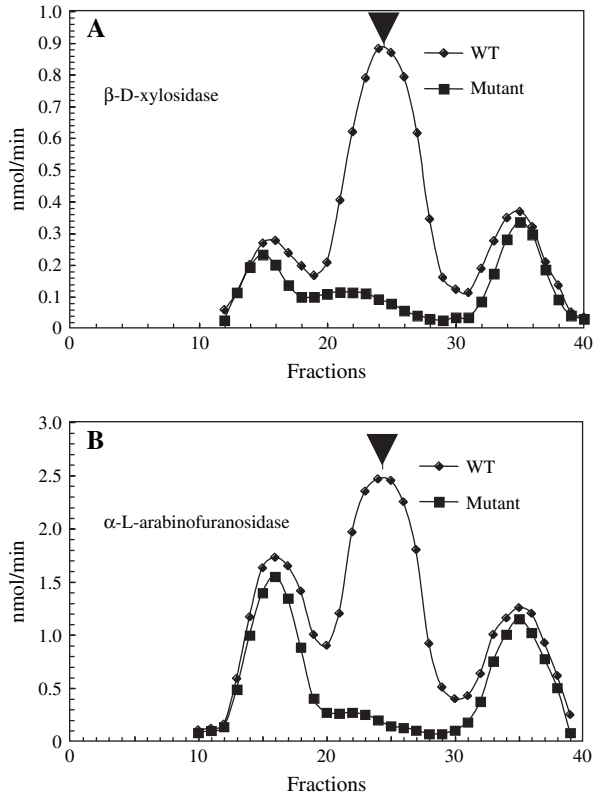

Fig. 8. Analysis of β-D-xylosidase (A) and α-L-arabinofuranosidase (B) activity in the *AtBX3* mutant using cation-exchange chromatography. Protein extracts obtained from wild-type (WT) and T-DNA mutant (Mutant) lines of *Arabidopsis* were analysed by CM-Sepharose chromatography. The protein extracts were dialysed in 25 mM Na-acetate buffer (pH 5.0) in the presence of 5% glycerol (v/v). Two millilitres (about 1.4 mg of protein) extract were loaded on a CM-Sepharose (Sigma) column (1.5 cm×4 cm) and eluted first with 20 mM Na-acetate buffer (pH 5.0) in the presence of 0.015% Triton X-100 (w/v), and then with the same buffer in the presence of a 0.1–0.5 M NaCl discontinuous gradient. One millilitre fractions were collected and 100 µl assayed for α-L-arabinofuranosidase and β-D-xylosidase activities at 37 °C for 60 min.

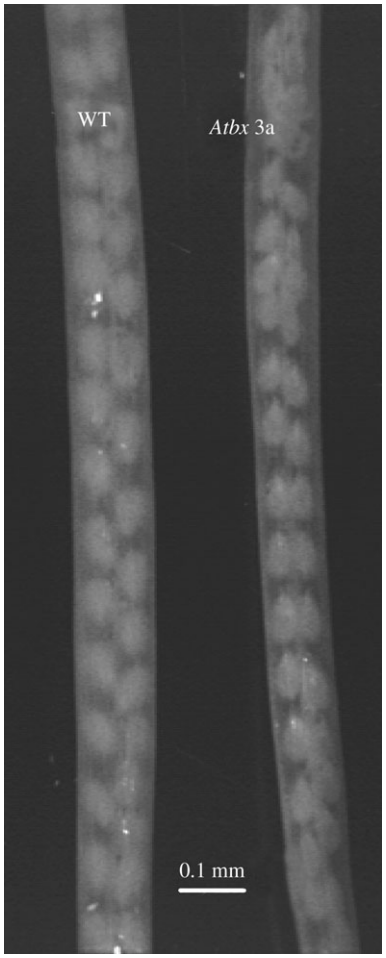

Fig. 9. Consequences of XYL3 absence on mutant lines. Comparison of siliques from wild type (WT) and *Atbx3* (*Atbx3a*). The photos were taken using a binocular microscope (NIKON SMZ-10A).

Table 4. *Weight and size of seeds of WT and* Atbx3a

The size reduction of the mutant seeds is significant (Student's test, $P < 0.05$).

Line	WT	*Atbx3a*
Weight of 20 seeds (µg)	329±15	322±12
Area of a seed (pixels)	805±14	750±18

seedlings (Lee *et al*., 2003) and XYL1 and ARAf from *Arabidopsis* stem tissues (Minic *et al*., 2004). It has been reported previously that the purified enzymes ARA-I and XYL1 have a discrepancy between the determined apparent molecular masses and those predicted from the cDNA size. It was demonstrated that ARA-I undergoes additional post-translation processing, as demonstrated experimentally by the cleavage of part of the peptide at the COOH terminal during enzyme maturation (Lee *et al*., 2003). Similar processing was suggested for the *Arabidopsis* XYL1 enzyme (Minic *et al*., 2004). By contrast to these enzymes, XYL3, which belongs to the same family of glycosyl hydrolases, has an apparent molecular mass, obtained by SDS-PAGE and gel filtration chromatography, similar to that calculated from the cDNAs after removal of the NH_2-terminal signal sequences. This absence of processing at the COOH-terminus side was also confirmed by the detection of a peptide corresponding to the COOH-terminus side by MALDI-TOF (Fig. 3). This suggests that, by contrast to ARA-I and XYL1, XYL3 does not undergo COOH post-translational processing.

Concerning α-L-arabinofuranosidase activities on natural polysaccharides, Beldman *et al*. (1997) have classified these enzymes into three types depending on their mode of action and substrate specificity. α-L-Arabinofuranosidases of type A preferentially degrade the (1→5)-α-L-arabinofuranooligosaccharide backbone arabinan. The second type of α-L-arabinofuranosidases, which are called type B, preferentially degrade L-Ara residues from the side chains of

arabinan or arabinoxylan. The third type of α-L-arabinofuranosidases, which are called type C, are specifically active on arabinosyl linkages of arabinoxylans. Recently, it has been suggested that two barley arabinoxylan hydrolases belong to the third type of α-L-arabinofuranosidases (Ferré *et al*., 2000; Lee *et al*., 2001). Similarly, ARAf from *Arabidopsis* is a homologue of the third type of α-L-arabinofuranosidase because, although it possesses a relatively broad substrate specificity, it prefers arabinoxylan as a substrate. By contrast to ARAf, XYL3 shows a higher substrate specificity for arabinan than for arabinoxylan. This substrate specificity was determined using natural arabinans consisting of (1→5)-α-linked residues, which are substituted at α(1→3) and α(1→2) with single or multiple-unit side chains (Bacic *et al*., 1988). The present results suggested that XYL3 can hydrolyse (1→3)-α-, (1→2)-α-linked side group residues and non-reducing terminal L-arabinofuranose residues of debranched (1→5)-α-L-arabinan backbone. This strongly suggests that XYL3 functions both as a type A and a type B α-L-arabinofuranosidase. Moreover, this finding supports the proposal that XYL3 may be involved in the hydrolysis of arabinan *in vivo*.

XYL3, in addition to releasing L-Ara, can also release D-Xyl from various natural and synthetic substrates. It has been shown that XYL3 released D-Xyl from arabinoxylan and xylan to a similar degree as ARAf which belongs to family 51 of glycoside hydrolases. Thus, it appears that there is no functional difference between these two enzymes concerning the release of D-Xyl from arabinoxylan and xylan. In addition, XYL3 can hydrolyse *p*NPX and *p*NPAf in a similar manner to α-L-arabinofuranosidases from both families 3 and 51 of plant glycosyl hydrolases, such as ARA-I, XYL1, and ARAf (Hrmova *et al*., 2001; Lee *et al*., 2003; Minic *et al*., 2004).

To date, three enzymes from family 3 of glycoside hydrolases with similar substrate specificity for synthetic substrates as XYL3 have been purified and characterized from germinated barley seeds, *Arabidopsis* stems, and Japanese pear (Lee *et al*., 2003: Minic *et al*., 2004; Tateishi *et al*., 2005). These enzymes could also hydrolyse various oligoarabinan and oligoxylan substrates. Additional data are needed concerning their specificities towards the natural polysaccharides, but all these enzymes are able to hydrolyse arabinan. However, the α-L-arabinofuranosidase from Japanese pear did not release D-Xyl and L-Ara from xylan and arabinoxylan (Tateishi *et al*., 2005). By contrast to this enzyme, XYL3 like the previously characterized XYL1 (Minic *et al*., 2004) is able to hydrolyse these polysaccharides. This difference may result from the different experimental approaches (TLC or HPAE chromatography) used to examine the releasing capacities of these enzymes. Therefore, it is possible that all these bifunctional α-L-arabinofuranosidases/β-D-xylosidases from family 3 of glycoside hydrolases have similar substrate specificities on natural polysaccharides.

As mentioned above, XYL3 can hydrolyse different natural polysaccharides to various degrees, and therefore has a broad substrate specificity. This broad substrate specificity has been reported for other cell wall-modifying plant glycosyl hydrolases (Leah *et al*., 1995; Kim *et al*., 2000; Sampedro *et al*., 2001; Steele *et al*., 2001; Rose *et al*., 2002; Lee *et al*., 2003; Minic *et al*., 2004). It is hypothesized that the multifunctional aptitudes of plant glycosyl hydrolases allows the effective modification of complex cell wall polysaccharides while restricting the number of enzymes required.

Immunocytochemical studies have shown that pectic polysaccharides, arabinan, and galactan, from carrot, potato, and pea cells are regulated in relation to cell proliferation, cell differentiation and cell development (Willats *et al*., 2001; McCartney and Knox, 2002; Oomen *et al*., 2002). The dynamic expression patterns for pectic polysaccharides such as (1→5)-α-L-arabinan and (1→4)-β-D-galactan have been correlated with developmental events (Willats *et al*., 2001). As *Arabidopsis* XYL3 can hydrolyse arabinan, this enzyme could participate in cell wall developmental processes. The pattern of expression of *AtBX3* is restricted to the seed endosperm during early-stage embryo development. The endosperm in *Arabidopsis*, as in many dicot species, is non-persistent, and is presumed to serve as a transient medium supporting embryonic morphogenesis and early maturation (Lopes and Larkins, 1993). The presence of arabinan, the best substrate for this enzyme, was demonstrated at the expression site of XYL3. Therefore, it is proposed that this enzyme releases arabinose from the pectin arabinan side chain and is involved in reserve mobilization for embryo development. The lack of this enzymatic activity had an impact on seed development since mature seed size was reduced. Furthermore, seed germination was delayed but seed viability was not affected.

Acknowledgements

This work was partly funded by the Genoplante program Af2001-009. We thank Benjamin Plumivage and Chrystelle Leroux for their excellent technical aid, Drs Christine Rochat and Bertrand Dubreucq for the gift of total RNA from different seed, flower, and silique developmental stages, Drs Leslie McCartney and Helen North for reading and improving this manuscript, and Dr Christian Malosse for mass spectrometric analyses.

References

Atkins GL, Nimmo IA. 1980. Currents trends in the estimation of Michaelis-Menten parameters. *Analytical Biochemistry* **104,** 1–9.

Bacic A, Harris PJ, Stone BA. 1988. Structure and function of plant cell walls. In: Preiss J, ed. *The biochemistry of plants*, Vol. 14. San Diego, CA: Academic Press, 297–371.

Baluska F, Parker JS, Barlow PW. 1992. Specific patterns of cortical and endoplasmic microtubules associated with cell growth rearrangements of F-actin arrays in growing cells of intact maize

root apex tissues: a major developmental switch occurs in the postmitotic transition region. *European Journal of Cell Biology* **72,** 113–121.

Beldman G, Schols HA, Pitson SM, Searle-van Leewen MJF, Voragen AGJ. 1997. Arabinans and arabinan-degrading enzymes. *Advances in Macromolecular Carbohydrate Research* **1,** 1–64.

Bouché N, Bouchez D. 2001. Arabidopsis gene knockout: phenotype wanted. *Current Opinion in Plant Biology* **4,** 111–117.

Boudet AM, Kajita S, Grima-Pettenati J, Goffner D. 2003. Lignins and lignocellulosics: a better control of synthesis for new and improved uses. *Trends in Plant Science* **8,** 576–581.

Bradford MM. 1976. A rapid and sensitive method for the quantification of microgram quantities of protein utilizing the principe of protein–dye binding. *Analytical Biochemistry* **72,** 248–254.

Coen ES, Romero JM, Doyle S, Elliott R, Murphy G, Carpenter R. 1990. Floricaula: a homeotic gene required for flower development in *Antirrhinum majus*. *Cell* **63,** 1311–1322.

Corpet F. 1988. Multiple sequence alignment with hierarchical clustering. *Nucleic Acids Research* **16,** 10881–10890.

Cosgrove DJ. 1997. Assembly and enlargement of the primary cell wall in plants. *Annual Review of Cell Developmental Biology* **13,** 171–201.

Doyle JJ, Doyle JL. 1990. Isolation of plant DNA from fresh tissues. *Focus* **12,** 13–15.

Estelle M, Somerville CR. 1987. Auxin-resistant mutants of *Arabidopsis thaliana* with an altered morphology. *Molecular and General Genetics* **206,** 200–206.

Ferré H, Broberg A, Duus JO, Thomsen KK. 2000. A novel type of arabinoxylan arabinofuranohydrolase isolated from germinated barley. *European Journal of Biochemistry* **267,** 6633–6641.

Fry SC. 2004. Primary cell wall metabolism: tracking the careers of wall polymers in living plant cells. *New Phytologist* **161,** 641–675.

Glushka JN, Terrell M, York WS, O'Neill MA, Gucwa A, Darvill AG, Albersheim P, Prestegard JH. 2003. Primary structure of the 2-*O*-methyl-alpha-L-fucose-containing side chain of the pectic polysaccharide, rhamnogalacturonan II. *Carbohydrate Research* **338,** 341–352.

Goujon T, Minic Z, El Amrani A, Lerouxel O, Aletti E, Lapierre C, Joseleau JP, Jouanin L. 2003. *AtBXL1*, a novel higher plant (*Arabidopsis thaliana*) putative beta-xylosidase gene, is involved in secondary cell wall metabolism and plant development. *The Plant Journal* **33,** 677–690.

Hazlewood GP, Gilbert HJ. 1998. Structure and function analysis of *Pseudomonas* plant cell wall hydrolases. *Progress in Nucleic Acid Research and Molecular Biology* **61,** 211–241.

Hrmova M, Varghese JN, De Gori R, Smith BJ, Driguez H, Fincher GB. 2001. Catalytic mechanisms and reaction intermediates along the hydrolytic pathway of a plant beta-D-glucan glucohydrolase. *Structure* **9,** 1005–1016.

Kim J-B, Olek AT, Carpita NC. 2000. Cell wall and membrane-associated exo- β-D-glucanases from developing maize seedlings. *Plant Physiology* **123,** 471–485.

Laemmli UK. 1970. Cleavage of the structural proteins during the assembly of the head of the bacteriophage T4. *Nature* **227,** 680–685.

Leah R, Kigel J, Svendsen I, Mundy J. 1995. Biochemical and molecular characterization of a barley seed β-glucosidase. *Journal of Biological Chemistry* **270,** 15789–15797.

Lopes MA, Larkins BA. 1993. Endosperm origin, development, and function. *The Plant Cell* **5,** 1383–1399.

Lee RC, Burton RA, Hrmova M, Fincher GB. 2001. Barley arabinoxylan arabinofuranosidases: purification, characterization and determination of primary structures from cDNA clones. *Biochemistry Journal* **356,** 181–189.

Lee RC, Hrmova M, Burton RA, Lahnstein J, Fincher GB. 2003. Bifunctional family 3 glycoside hydrolases from barley with α-L-arabinofuranosidase and β-D-xylosidase activity. *Journal of Biological Chemistry* **278,** 5377–5387.

Lincold C, Long J, Yamaguchi J, Serikawa K, Hake S. 1994. A knotted1-like homeobox gene in *Arabidopsis* is expressed in the vegetative meristem and dramatically alters leaf morphology when overexpressed in transgenic plants. *The Plant Cell* **6,** 1859–1876.

Manin C, Shareek F, Morosoli R, Kluepfel D. 1994. Purification and characterization of an alpha-L-arabinofuranosidase from *Streptomyces lividans* 66 and DNA sequence of the gene (*adf*A). *Biochemical Journal* **302,** 443–449.

McCartney L, Knox JP. 2002. Regulation of pectic polysaccharide domains in relation to cell development and cell properties in the pea testa. *Journal of Experimental Botany* **53,** 707–713.

Minic Z, Rihouey C, Do C-T, Lerouge P, Jouanin L. 2004. Purification and characterization of enzymes exhibiting β-D-xylosidase activities in stem tissues of *Arabidopsis*. *Plant Physiology* **135,** 867–878.

Nakai K, Horton P. 1999. PSORT: a program for detecting sorting signals in proteins and predicting their subcellular localization. *Trends in Biochemical Sciences* **24,** 34–36.

Nielsen H, Engelbrecht J, Brunak S, Heijne G. 1997. A neural network method for identification of prokaryotic and eukaryotic signal peptides and prediction of their cleavage sites. *International Journal of Neural Systems* **8,** 581–599.

Obel N, Porchia AC, Scheller HV. 2002. Dynamic changes in cell wall polysaccharides during wheat seedling development. *Phytochemistry* **60,** 603–610.

Oomen RJ, Doeswijk-Voragen CH, Bush MS, *et al.* 2002. *In muro* fragmentation of the rhamnogalacturonan I backbone in potato (*Solanum tuberosum* L.) results in a reduction and altered location of the galactan and arabinan side-chains and abnormal periderm development. *The Plant Journal* **30,** 403–413.

Popper ZA, Fry SC. 2003. Primary cell wall composition of bryophytes and charophytes. *Annals of Botany* **91,** 1–12.

Puls J, Schuseil J. 1993. Hemicelluloses: relationship between structure and enzymes required for hydrolysis. In: Coughlan MP, Hazlewood JP, eds. *Hemicellulose and hemicellulase*. London: Portland, 1–27.

Rahman AK, Kato K, Kawai S, Takamizawa K. 2003. Substrate specificity of the α-L-arabinofuranosidase from *Rhizomucor pusillus* HHT-1. *Carbohydrate Research* **338,** 1469–1476.

Reiter WD. 2002. Biosynthesis and properties of the plant cell wall. *Current Opinion in Plant Biology* **5,** 536–542.

Ridley BL, O'Neill MA, Mohnen D. 2001. Pectins: structure, biosynthesis, and oligogalacturonide related signaling. *Phytochemistry* **57,** 929–967.

Rose JK, Braam J, Fry SC, Nishitani K. 2002. The XTH family of enzymes involved in xyloglucan endotransglucosylation and endohydrolysis: current perspectives and a new unifying nomenclature. *Plant Cell Physiology* **43,** 1421–1435.

Saha BC. 2000. Alpha-L-arabinofuranosidases: biochemistry, molecular biology, and application in biotechnology. *Biotechnology Advances* **18,** 403–423.

Sambrook J, Fritsch E, Maniatis T. 1989. *Molecular cloning: a laboratory manual*, 2nd edn. Cold Spring Harbor, NY: Cold Spring Harbor Laboratory Press.

Sampedro J, Sieiro C, Revilla G, Gonzalez-Villa T, Zarra I. 2001. Cloning and expression pattern of a gene encoding an alpha-xylosidase active against xylogucan oligosaccharides from *Arabidopsis*. *Plant Physiology* **126,** 910–920.

Santoni V, Vinh J, Pflieger D, Sommerer N, Maurel C. 2003. A proteomic study reveals novel insights into the diversity of

aquaporin forms expressed in the plasma membrane of plant roots. *Biochemical Journal* **373,** 289–296.

Steele NM, Sulova Z, Campbell P, Braam J, Farkas V, Fry SC. 2001. Ten isoenzymes of xyloglucan endotransglycosylase from plant cell walls select and cleave the donor substrate stochastically. *Biochemical Journal* **355,** 671–679.

Stolle-Smits T, Beekhuizen JG, Kok MT, Pijnenburg M, Recourt K, Derksen J, Voragen AG. 1999. Changes in cell wall polysaccharides of green bean pods during development. *Plant Physiology* **121,** 363–372.

Tateishi A, Mori H, Watari J, Nagashima K, Yamaki S, Inoue H. 2005. Isolation, characterization, and cloning of α-L-arabinofuranosidase expressed during fruit ripening of Japonese pear. *Plant Physiology* **138,** 1653–1664.

Willats WGT, Marcus SE, Knox JP. 1998. Generation of a monoclonal antibody specific to (1→5) α-L-arabinan. *Carbohydrate Research* **308,** 149–152.

Willats WG, McCartney L, Mackie W, Knox JP. 2001. Pectin: cell biology and prospects for functional analysis. *Plant Molecular Biology* **47,** 9–27.